2022 8th International Conference on Control, Decision and Information Technologies
CoDIT'22 | Istanbul, Turkey / May 17-20, 2022

Traffic flow prediction under non-recurrent events using microscopic simulation

Benchawan Wiwatanapataphee*, Weenakorn Ieosanurak†, Yong Hong Wu‡, Graham Jacoby§, Xinguang Zhang¶
*‡¶School of Electrical Engineering, Computing and Mathematical Sciences, Curtin University;
† Department of Mathematics, Faculty of Science, Khon Kaen University, Thailand
§ Main Roads Western Australia, Perth WA, Australia
*b.wiwatanapataphee@curtin.edu.au, †weenie@kku.ac.th, ‡y.wu@curtin.edu.au,
§graham.jacoby@mainroads.wa.gov.au, ¶xinguang.zhang@curtin.edu.au

2022 8th International Conference on Control, Decision and Information Technologies (CoDIT) | 978-1-6654-9607-0/22/$31.00 ©2022 IEEE | DOI: 10.1109/CODIT55151.2022.9804134

***Abstract*—This paper focuses on the microsimulation of traffic flow on freeways with on-ramps, off-ramps and bottlenecks. The road network model with many vehicle routes is constructed based on the detector flow data recorded every minute on each freeway lane. A comparative study evaluates the effectiveness of the proposed traffic flow model. It is noted that the model can successfully capture the essential features of traffic flow on the freeway. With the calibrated model, various numerical experiments are then conducted to investigate the impact of ramp metering (RM) and variable speed limit (VSL) on average waiting time, average travel time, average traffic speed, and the total number of running vehicles over certain period of time on the road network. The results indicate that the RM and VSL control can significantly improve traffic flow on the freeway.**

***Index Terms*—Microscopic traffic flow model, Variable speed limits, Ramp metering, SUMO traffic simulator**

I. Introduction

Freeways have been used in many cities worldwide as an important urban road network component to reduce traffic jams and improve transportation efficiency. However, due to rapid economic growth in recent years, traffic congestion on freeways has been a major transportation issue in urban cities in many countries, especially during the traffic rush hours and non-recurrent event periods. Traffic congestion causes travel delay and has severe economic and environmental implications due to increased harmful carbon dioxide emissions.

Over the last few decades, many traffic management strategies [1] have been developed to balance freeway demand and capacity to reduce traffic congestion. These strategies include Ramp Metering (RM), Variable Speed Limits (VSL), Closed-Circuit TeleVision (CCTV) monitoring, emergency lane, and guideline system. Among these strategies, RM and VSL controls are being widely used today. RM is used to alter the number of vehicles that are allowed to enter the freeway. The more congested the main freeway is, the longer red times to the traffic signals leading to fewer vehicles entering the Freeway. VSL technology is aimed to provide waiting drivers more opportunity to join the main road at a slower speed to ease congestion and reduce the risk, incidence and severity of road crashes.

Several RM and VSL approaches have been proposed for motorway traffic control. The ramp metering algorithms can be classified into localized and coordinated systems. The localized RM strategies regulate a single on-ramp as an independent system. The coordinated RM algorithms assign metering rates to each metered on-ramp and regulate a facility with multiple on-ramps that experience recurring congestion. Popular local ramp metering strategies include the Asservissement Linéaire d'Entrée Autoroutiére (ALINEA) [2] and its extensions [3]. For the coordinated RM algorithms, various algorithms have been developed such as the Stratified Zone Metering (SZM) algorithm [4], the Heuristic Ramp-metering CoOrdination (HERO) algorithm [5], [6], and the System-Wide Adaptive Ramp Metering (SWARM) algorithm [7]. In recent years, the ALINEA and HERO algorithms have been widely used for RM control.

For the local ALINEA strategy, the metering rate at the previous time step and the downstream traffic density are used as the input to determine the metering rate for the current time step k. In brief, at the ramp-mainline merging section, the ALINEA feedback control law [5] can be expressed by

$$\begin{aligned} \tilde{q}_i^k &= \tilde{q}_i^{k-1} + K_R\left(\tilde{\rho}_i - \rho_i^k\right) \quad (1) \\ \text{or } \tilde{q}_i^k &= \tilde{q}_i^{k-1} - K_P\left(\rho_i^k - \rho_i^{k-1}\right) + K_R\left(\tilde{\rho}_i - \rho_i^k\right) \end{aligned}$$

where $\tilde{q}_i^k$ is the local metering rate of the on-ramp i, $\tilde{\rho}_i$ denotes the desired traffic density, ρ_i^k is the measurement of the traffic density from the merging segment, and K_P and K_R are positive regulator parameters. Papamichail [5] proposed a linked ramp-metering scheme based on the combination of ALINEA and HERO algorithms for the linked control of the inflow from two (or more) consecutive on-ramps to the freeway mainstream. The on-ramp outflow rate, q_i^k, may be determined by

$$q_i^k = \max\left\{\tilde{q}_i^k,\ \hat{q}_i^k\right\}. \quad (2)$$

The term $\tilde{q}_i^k$ in the above equation is the local metering rate determined by either Equation $(1)_1$ or Equation $(1)_2$ and the term $\hat{q}_i^k$ is the ramp outflow rate determined by

$$\hat{q}_i^k = d_i^{k-1} - \frac{1}{T_c}\left[M_i - m_i^k\right], \quad (3)$$

where M_i and m_i denote respectively the maximum queue length and the current queue length of the on-ramp i, and d_i represents the on-ramp arriving demand rate.

The performance of RM algorithms has been evaluated numerically through either macroscopic models [2], [5], [8]–[16] or microscopic models [3], [6], [7], [17]–[20]. Compared to the macroscopic traffic simulation model, microscopic models are regarded as the most thoughtful approaches, particularly in situations where detailed simulation of vehicle-road and vehicle-vehicle interactions are required. Various microscopic traffic simulators such as PARAMICS, VISSIM, AIMSUN and SUMO have been widely used to perform empirical studies. Chu et al. [20] evaluated adaptive ramp-metering algorithms in a PARAMICS simulation environment throughout the I-405 Freeway in California, under both recurrent congestion and incident scenarios. Abuamer et al. [17] investigated the ALINEA ramp metering strategy and VSL control on merging flows on an Istanbul D-100 freeway using the VISSIM microscopic simulator. Mohammad and Kondyli [6] used the VISSIM simulator to evaluate three simulated scenarios of no control, ALINEA, and HERO on travel time along an 8-mile-long freeway in Kansas City. Amini et al. [18] evaluated the HERO-based ramp metering algorithm using AIMSUN simulator. Minoarivelo [21] adapted SUMO to simulate a crossroad under the control of an intelligent traffic light. Although the RM and VSL control has effectively reduced congestion and improved safety, the impact of the RM-VSL control on travel time, waiting time, number of running vehicles, and mean speed has not been extensively studied.

This paper aims to evaluate the impact of RM and VSL controls on travel time, waiting time, total number of running vehicles and mean speed, with a particular application focus on traffic control and management for the Kwinana Freeway between Roe Highway and Narrows Bridge. For achieving this goal, based on the existing traffic flow models, a more general microscopic model is established taking into account the road capacity described by the fundamental diagram, the variable speed limits and the ramp metering control. Then by using real-world traffic flow data, a base model of the test site, the Kwinana freeway between Roe Highway and Narrows Bridge, is calibrated with the microscopic model implemented in the SUMO simulator to reproduce real-world traffic conditions. With the calibrated model, the RM and VSL control strategies are then implemented and various numerical experiments are designed to evaluate the impact of the control strategies.

The rest of the paper is organized as follows. In Section II, the microscopic model established for this study is presented. The road network used in this study and its fundamental properties, drawn from the real-world traffic flow data, are given in Section III. Calibration of the base model is shown in Section IV, demonstrating the matching of simulation results with measurement data and also the characteristics of traffic flow in the freeway network. Numerical investigation of the impact of RM and VSL control strategies is given in Section V, followed by the conclusions in Section VI.

II. Traffic Flow Simulation Model

In microscopic models, traffic flow on multi-lane networks is simulated by modelling the movements of individual vehicles. For different models, different assumptions on real driving behaviour are made, such as keeping a safe distance from the leading vehicle or driving at an optimal speed in a certain sense. The intelligent driver model (IDM) is an accident-free model that can provide realistic acceleration profiles for traffic flow on freeways. In this study, we establish a more general model for the study of traffic flow on freeway networks based on the IDM and the default microscopic model in SUMO.

The default microscopic model in SUMO is based on the work in [22] in which the desired speed for each individual vehicle at the time instant k (i.e. $t = k\triangle t$) is given by

$$v^k = \min\left\{v^k_{safe},\ v^{k-1} + \hat{a}\triangle t,\ \hat{v}\right\}, \tag{4}$$

where $\hat{a}$ and $\hat{v}$ are respectively the maximum acceleration and maximum speed of the vehicle, and v^k_{safe} is the safe speed of a vehicle which can be determined by

$$v^k_{safe} = v^k_\alpha + \left(g^k - \tau v^k_\alpha\right) / \left(\frac{\bar{v}}{b} + \tau\right), \tag{5}$$

in which v^k_α represents the speed of the leading vehicle, $\bar{v}$ is the average speed, b is the comfortable braking deceleration depending on the average speed, τ is the driver's reaction time, and g^k is the gap to the leading vehicle defined by

$$g^k = x^k_\alpha - x^k - \ell, \tag{6}$$

in which x^k_α and x^k denote respectively the positions of the leading vehicle and the follower vehicle, and ℓ is the length of the leading vehicle.

Based on the above work and the IDM model, taking into account the variable speed limit control as well as the fundamental diagram obtained from real-world traffic data, we propose the following generalized IDM model for the desired vehicle speed,

$$v^k = \min\left\{v^k_{safe},\ v^{k-1} + a^{k-1}\triangle t,\ \hat{v},\ v_e,\ v_\ell\right\}, \tag{7}$$

where v_e denotes the equilibrium speed obtained from the fundamental diagram from real-world traffic flow data, v_ℓ denotes the imposed variable speed limits, and $a = \dot{v}$ is defined by

$$a^k = \begin{cases} \hat{a}\left(1 - \left(\frac{v^k}{v_{opt}}\right)^\delta - \left(\frac{g^k_{safe}}{g^k}\right)^2\right) & \text{if } v^k < v_e; \\ -b\left[1 - \left(\frac{v_e}{v^k}\right)^\delta\right] & \text{if } v^k \geq v_e. \end{cases} \tag{8}$$

In Equation (8), the formula for $v(k) \geq v_e$ is for decelerating the vehicle with higher maximum speed, the formula for $v(k) < v_e$ is the intelligent driver model (IDM) in which v_{opt} is the optimal speed, δ and b are model parameters, and g^k_{safe} is the dynamic safe gap defined by

$$g^k_{safe} = \begin{cases} g_{min} + v^k \cdot T^k + \frac{v^k \triangle v}{2\sqrt{\hat{a}\cdot b}} & \text{if } b > b_k \\ \frac{(v^k)^2}{2\sqrt{\hat{a}\cdot b}} & \text{if } b < b_k \end{cases} \tag{9}$$

where g_{min} denotes the minimum safe gap, $T(k)$ is the safe time gap to the leading vehicle at time instant k, and $\triangle v$ is the

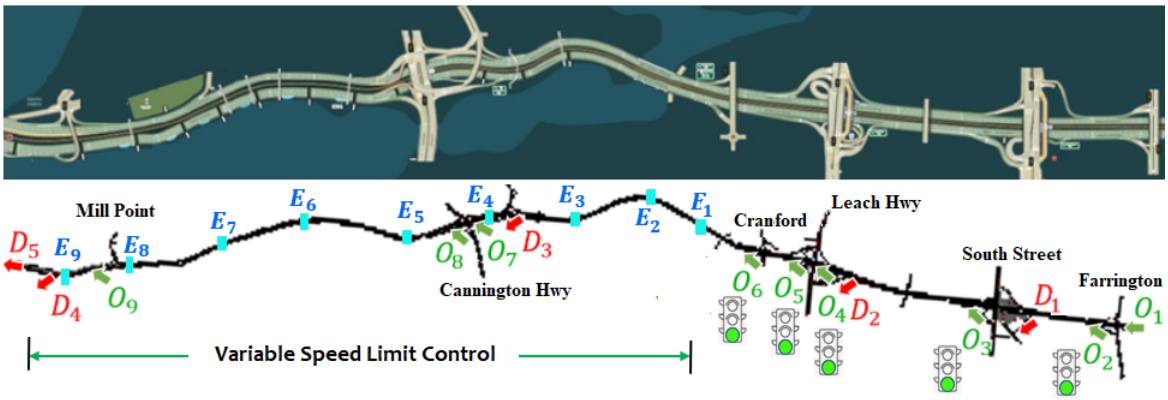

Fig. 1. The Smart Kwinana Freeway northbound with incoming flows $(O_1, \ldots, O_9)$, outgoing flows $(D_1, \ldots, D-9)$, five ramp meters $(O_2, \ldots, O_6)$, and the vehicle detector signs for speed limit control $(E_1, \ldots, E_9)$ used for model calibration.

speed difference to the leading vehicle, $\triangle v = v(k) - v_\alpha(k)$. In Equation (9), $b_k = (v^k)^2/2g^k$ is the kinematic deceleration to avoid collision; $b > b_k$ for regular condition and $b < b_k$ for critical condition [23].

Remark: The substitution of the maximum acceleration $\hat{a}$ in (4) by the IDM will make the model more realistic as both the optimal speed v_{opt} and the safe gap have been taken into account in the IDM. In addition, the term v_e in (7) takes into account the characteristics of freeway described by the fundamental diagram obtained from real traffic data, and the addition of the term v_ℓ makes it possible to mimic the situation with variable speed limits.

As traffic congestion often occurs at the on-ramp merging areas, controlling the merging between the on-ramp vehicles and the vehicles close to the on-ramp via ramp metering is important for improving traffic flow conditions. The upstream vehicle speed near the on-ramp can be expressed by

$$u_i^k = \min\left\{w_i^k, v_i^k, u_\ell\right\}, \tag{10}$$

where w_i^k is the speed of the vehicles on the on-ramp downstream area, v_i^k is the speed of vehicles from on-ramp i entering the freeway, and u_ℓ is the upstream speed limit. Based on the ALINEA and HERO algorithms, from Equation (1)-(4), v_i^k can be determined by

$$v_i^k = \min\left\{\frac{q_i^k}{\rho_i^k}, \hat{v}_i\right\}, \tag{11}$$

where ρ_i^k denotes the traffic density on on-ramp i and $\hat{v}_i$ is the on-ramp speed limit.

As freeway road networks have multi-lane roads, a vehicle might require changing lane if the potential new target lane is more attractive and the change can be performed safely under heavy traffic conditions. The lane-changing model in SUMO is applied in this study. Here, we consider lane-changing on merging and bottleneck areas. Whenever an IDM vehicle advances to the next lane, the data-structure of the road network is updated.

By solving the coupled differential equations of the above IDM for v_k and a^k, new position and new gap of an IDM vehicle at an update time $k+\triangle t$ can be respectively computed by the following equations:

$$x^{k+1} = x^k + v^k \triangle t + \frac{1}{2}a^k(\triangle t)^2, \tag{12}$$

$$g^{k+1} = x_\alpha^{k+1} - x^{k+1} - \ell. \tag{13}$$

III. Road Network Model and Traffic Flow Characteristics

In this paper, we aim to investigate the impact of variable speed limits and ramp metering for the freeway network in Perth. This involves the development of simulation model including SUMO script sources, a road network computer model, calibration of the model, and numerical investigation. In this section, we present the road network computer model of the Kwinana Freeway used for the investigation, and the characteristics of the traffic flow data used for calibration of the model.

A. Road network computer model

In Perth, smart freeway technology has been used on the Kwinana Freeway between Roe Highway and Narrows Bridge. It is the first smart Freeway in Western Australia upgraded from the existing freeway. The upgrading includes converting the existing emergency lane between Canning Highway and the Narrows Bridge into a full-time traffic lane completed in 2021, installing CCTV cameras to enable continual traffic monitoring and management completed in 2019, changing speed limits whenever needed and displaying lane closure information via overhead electronic signs completed in 2020 and installing five ramp meters with coordinated signals at Farrington Road, South Street, Leach Highway and Cranford Avenue on-ramps.

The road network of Kwinana Freeway between Roe Highway and Narrows Bridge has a total length of 13.089 kilometres, as shown in Fig. 1. It is firstly extracted from the Open StreetMap and then converted into an XML file.

B. Traffic flow characteristics

Two sets of historical traffic data have been used in this study, including edge-scaled data and lane-scaled data of traffic volume, speed and occupancy. These data were gathered every minute by Vehicle Detector Sites (VDS) placed on the Kwinana Freeway between Roe Highway and Narrows bridge.

The data have been processed and analyzed to show the characteristics of freeway traffic flow. It is noted that when the traffic density is low, say $\rho < \rho_c$, vehicles move at free-flow speed v_f, and an increase of the density decreases the speed of the roadway. When $\rho_c < \rho < \rho_{jam}$, the speed-density relationship is linear with a negative slope. Based on this traffic flow characteristics and the work in [24], the jam density is about seven times of the critical density. We can thus define a density parameter $\gamma = \frac{7\rho_c - \rho}{6\rho_c}$, and the equilibrium speed is modelled by a piecewise function as follows:

$$v_e = \begin{cases} v_f, & 0 \le \rho \le \rho_c; \\ \gamma v_f, & \rho_c < \rho \le \rho_{jam}. \end{cases} \quad (14)$$

For multi-lane road network, we also use the lane-scaled data available on 31 October 2018 to determine path-scaled routes of the traffic system. In SUMO, simulated data were recorded by two types of virtual detectors:

1) Multi-entry/multi-exit (e3) detector covering a short cross-section of an edge which corresponds to an edge-scaled detector in the actual world situation;
2) Lane (e1) detector which equates to a single loop detector in practice.

Totally, 14 e3-detectors and 156 e1-detectors are used in the computer model corresponding to the actual VDS placed between Roe Highway and Narrows Bridge of the Kwinana Freeway.

IV. Model Calibration

Numerical experiments are conducted utilizing the SUMO software package. SUMO, developed initially by the German Aerospace Centre, uses software tools for microscopic traffic simulation, and has been successfully applied in the study of real-world traffic flow in several projects [25]–[30]. It provides the flexibility for users to extend or update the software tools to include new traffic flow models and new traffic control strategies such as RM and VSL. The simulation method presented in Section two has been implemented in SUMO for this study.

To calibrate the simulation model, the numerical results obtained with different parameter values are compared with real-world traffic data. In this work, the road network with unmanaged control of ramp metering is considered for the calibration purpose. Considering the data across all lanes and also on each lane, it is found that flow rate and speed vary with lane. Fig. 2 shows the profiles of flow rate (veh/min) and their Root Mean Square Error (RSME) across all lanes of the observed data (navy lines) and the simulation results (green lines) from the detector E_1 to E_9 between Cranford Avenue and Narrows Bridge (see Fig. 1). The RMSE values for traffic

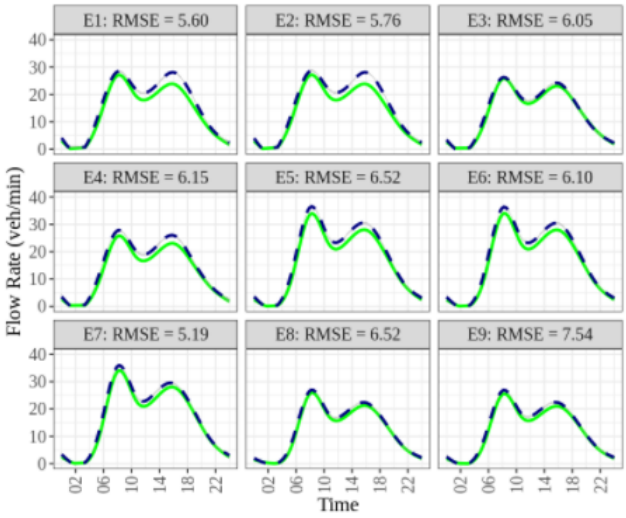

Fig. 2. Measured data (blue color) and simulation results (green color) of traffic flow rate from the induction loop detector E_1 to the detector E_9 between Cranford Avenue and Narrows Bridge.

flow across all lanes are between 5.19 and 7.54. It indicates that the simulated data (green lines) of the flow rate across all lanes agree well with the observed data (navy lines).

V. Numerical Investigation

With the calibrated model, various numerical experiments are conducted to investigate the impact of VSL and RM control strategies on traffic flow for the Kwinana Freeway between Roe Highway and Narrows Bridge in Perth. Our microscopic traffic simulation is 24 hours with 86400 incremental time steps of step size $\triangle t = 1$ second. All model parameters are determined through the calibration process. We obtain the following parameter values: the maximum acceleration a is 1.5 m/s^2, the exponent δ is 4, the minimum gap g_0 is 2 m, and the comfortable deceleration rates b is 2.67, 2.53 and 2.55 m/s^2 respectively for the mean speed ranges of $60-70$, $70-80$ and $80-100$ km/h.

Busy on-ramp, and off-ramp roads as well as lane drop may create a weaving bottleneck, resulting in traffic congestion on the freeway. Controlling freeway traffic is one of the essential transportation infrastructures. Various control systems have been used on the freeways including RM and VSL controls. As the Freeway can provide unrestricted access for road users without introducing RM and VSL controls during non-rush hours, the impact of RM and VSL controls during rush hours on freeway traffic is investigated. This study applies the linked ramp-metering scheme based on the ALINEA and HERO algorithms [5] at five on-ramp roads on Farrington road, South Street, Leach Highway (2 TLS) and Cranford Avenue.

The RM with a cycle length of 120 seconds and 90 seconds is used to manage traffic flow entering the Freeway during rush hours in the morning (6:00-10:00 am) and the afternoon (14:00-16:00 pm). The traffic lights go on a green cycle for 15 seconds, yellow for 5 seconds, and a red of 100 seconds during the rush hours, and a process of green for 80 seconds,

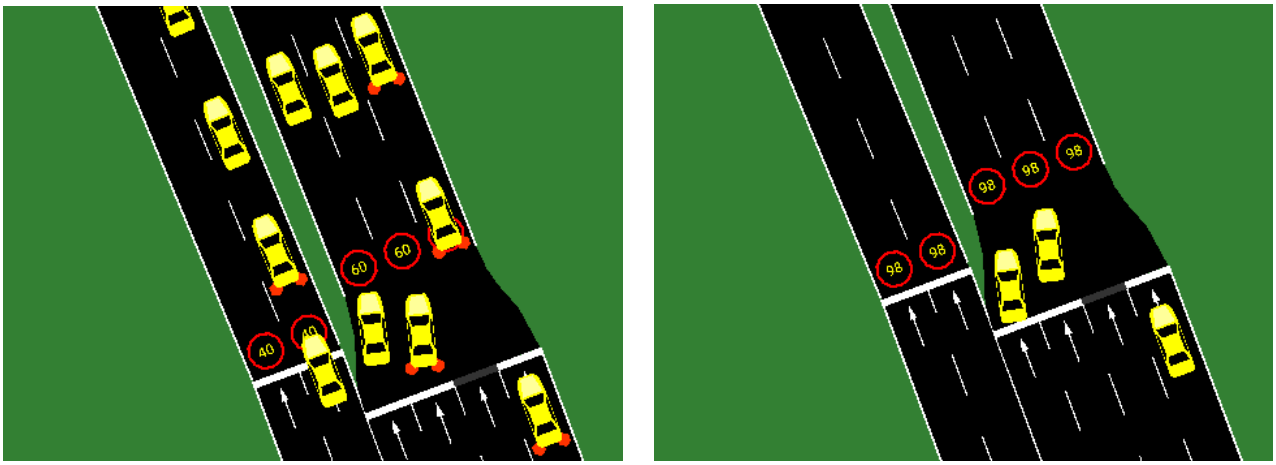

(a) rush hours (b) non rush hours

Fig. 3. VSL signs for the 2-lane on-ramp road and the 3-lane mainline next to Cannington Highway during different periods of time: (a) the rush hours; (b) non rush hours.

yellow for 5 seconds, followed by red for 5 seconds during non-rush hours. The VSL control is used to control both on-ramp and mainline traffic between Cranford Avenue and Narrows Bridges. In this study, we choose the mainline VSL control of 60 and 90 km/h and the on-ramp VSL control of 40 and 60 km/h during rush hours in this study. Fig. 3 shows the VSL signs at the 2-lane on-ramp (O_8 in Fig. 1) and the 3-lane mainline next to Cannington Highway during the morning peak hours between 6:00 and 10:00 (left), and the time intervals from 0:00 to 6:00, and 10:00 to 24:00 (right). The estimation of vehicle routes and traffic demand based on detector data can be formulated by

$$\sum_{i}^{I} p_{ij} O_i \;=\; D_j;\; \sum_{j} p_{ij} = 1, \quad j = 1, \ldots, J \tag{15}$$

where p_{ij} denotes the proportion of trip from the ith origin (source) flowing to the jth destination (sink), O_i and D_j are respectively the ith source and jth sink counts, and I and J represent total numbers of source and sink detectors, respectively.

In the road network, there are 29 possible O-D routes. Based on real-time detector data of on-ramp arrival rate (demand) $d_{i,r}^t$ and off-ramp outflows (supply) s_j^t at time t, the proportions of trips from the ith origin (source) to the jth destination (sink) of the road network model can be determined by a non-linear constrained optimization problem:

$$\begin{aligned} &\min \textstyle\sum_{i=1}^{9} \sum_{j=1}^{5} \left(d_{i,r}^t p_{ij} - s_j^t\right)^2,\ \tau \le t \le t_n \\ \text{subject to} \quad &\textstyle\sum_{j=1}^{5} p_{ij} = 1, \text{ for all } i;\ 0 \le p_{ij} \le 1, \\ &p_{i1}|_{i=3}^{9} = p_{i2}|_{i=4}^{9} = p_{i3}|_{i=7}^{9} = 0. \end{aligned} \tag{16}$$

The optimal decision variables p_{ij} (the proportion of trips from O_i to D_j minimizing the objective function) are then obtained by solving the constrained optimization problem.

To investigate the effect of RM and VSL control on relieving congestion caused by a road incident, the green duration of those five ramp meters and the speed limits at a time step k are determined by

$$G_i^k = \frac{q_i^k}{q_s^k} C_i; \quad V_i^k = \beta_i^k v_{f,i}, \tag{17}$$

where q_i^k is the ramp flow into a multilane freeway defined in equation (2), q_s^k is the ramp capacity flow (saturation flow), C_i is the cycle length of ramp metering signals and β_i is the VSL parameter.

For a vehicle route ξ, we let ℓ_ξ and N_ξ be respectively the driving (journey) distance, and the number of vehicles passing through a vehicle route, v_f be the free-flow speed or the desired speed of drivers in low volume conditions. The degree of traffic congestion can be measured by three indicators: average travel speed, average travel time, and average delay. For all motorized vehicles in a vehicle route (the same time and on the same journey), the speed (v_ξ), the time spent (T_ξ) and the time loss (τ_ξ) due to on-ramp traffic lights and heavy bottleneck traffic can be respectively estimated by

$$v_\xi = \frac{\ell_\xi}{T_{avg}}; T_\xi = \frac{\ell_\xi}{V_{avg}};\ \tau_\xi = \ell_\xi \sum_{n=1}^{N_\xi} \left(\frac{1}{v_n} - \frac{1}{v_f}\right), \tag{18}$$

where $T_{avg} = (\sum_{n=1}^{N_\xi} T_n)/N_\xi$ denotes average time spend, $V_{avg} = (\sum_{n=1}^{N_\xi} v_n)/N_\xi$ is average speed, T_n is the time required to pass the nth vehicle and v_n is the vehicle speed.

For clear explanation, the model with unmanaged strategy is called the unmanaged model, the one with the on-ramp speed of 40 km/h and the mainline speed of 60 km/h is called the VSL-60-40-RM model, and the one with the on-ramp speed of 60 km/h and the mainline speed of 90 km/hr is called the VSL-90-60-RM model.

Fig. 4 presents the average waiting time, the travel time, the number of running vehicles over time and the mean speed obtained from the model with three different traffic management strategies: the unmanaged model (solid line), the VSL-60-40-RM model (dotted line) and the VSL-90-60-RM

model (dashed line). From Fig. 4(a), the profiles of waiting time for the VSL-60-40-RM strategy and the VSL-90-60-RM strategy have the same pattern. Both profiles (dotted line and dashed line) stay at around the zero level in the early morning (0:00-6:00 am, start going up sharply after 6:00 am to reach its peak values of $125s$ (dotted line) and $95s$ (dashed line) at 10:00 am, then go down to $100s$ (dotted line) and 75s (dashed line) at 12:00 pm. For the unmanaged model, its waiting time profile (solid line) stays at the zero level in the early morning (0:00 am - 6:00 am), starts going up quickly after 6:00 am to reach its peak values of $75s$ at 10:00 am, and then goes down to $70s$ at 11:00 am. From Fig. 4(b), the average travel times by the three different management strategies are almost in the same pattern. Travel time profiles stay at the same value of about $400s$ for the unmanaged model from 1:00 am to 6:00 am and about $300s$ for the two managed models during this period. The travel time profile of the unmanaged model increases quickly to about $775s$ at 12:00 pm and stays at the value between $750s$ and $775s$ from 12:00 pm to 12:00 am. For the two managed models, the travel time profiles increase dramatically to $550s$ (dotted line) and $450s$ (dashed line) at 10 am, and then decrease gradually to about $400s$.

From Fig. 4(c), all profiles of the number of running vehicles stay almost at the same level in the early morning between midnight and 4:30 am. For the two managed strategies, the profiles start going up after 4:30 am with a high growth rate to peak values of 2200 vehs at 9:00 am (dotted line) and 1950 vehs at 8:00 am (dashed line). After 11:00 am, both profiles have almost the same shape with the peak value of around 1200 vehs at 5:00 pm. For the unmanaged model, there are three peak values respectively at 3000 vehs at 8:00 am, 2350 vehs at 4:00 pm and 2300 vehs at 5:00 pm. From Figure 4 (d), the mean speeds of the VSL-60-40-RM model (dotted line) and the VSL-90-60-RM model (dashed line) vary between 80 and 100 km/h in early morning (0:00-6:00 am), decline quickly to 35 km/h (dotted line) and 40 km/h (dashed line) at 7:00 am. Comparing to the VSL-90-60-RM model, the mean speed of the VSL-60-40-RM model is higher during the period of 7:00 to 9:00 pm. From 9:00 pm to midnight, both profiles have the same shape. For the unmanaged model, the mean speed varies between 50 and 80 km/h in the early morning, drops quickly to 20 km/h at 8:00 am. The results illustrate that the VSL-90-60-RM control strategy yields a higher speed during the rush hours. The RM and VSL control strategies improve traffic speed and reduce average travel time all day. In the VSL-60-40-RM model (dotted line), road users spend more time on the Freeway. The VSL-90-60-RM model (dashed line) provides a shorter travel time all day. The shorter the average travel time is, the smoother the traffic will be. The longer the average travel time is, the more severe the traffic congestion will be.

VI. Conclusions

Based on the existing traffic flow model, a more general microscopic model has been established which can predict all the necessary traffic dynamics. Using real-world traffic flow data, the microscopic model implemented in SUMO has been calibrated. The results indicate that the established model coupled with the SUMO simulation package is able to reproduce real-world traffic flow phenomena. The RM and VSL control strategies have been successfully implemented in the model, and numerical investigations show that the RM and VSL control strategies can significantly improve the traffic flow, including reducing mean travel time and increasing mean vehicle speed, as well as reducing the number of vehicles on the road network.

VII. Acknowledgments

This research is supported by the Australian Research Council through the linkage project funding scheme (project LP170100341). The authors would like to thank the Main Roads Western Australia (MRWA) for providing traffic data for this research, and also would like to acknowledge the Road and Maritime Service NSW and the Australia Sustainable Environment National Research Centre for their support of the project.

References

[1] S. Hoogendoorn and P. Bovy, "State-of-the-art of vehicular traffic flow modelling," *Proceedings of the Institution of Mechanical Engineers, Part I: Journal of Systems and Control Engineering*, vol. 215, no. 4, pp. 283–303, 2001.

[2] M. Papageorgiou, H. Hadj-Salem, and F. Middelham, "Alinea local ramp metering: Summary of field results," *Transportation Research Record: Journal of the Transportation Research Board*, 1997.

[3] K. Shaaban, M. Khan, and R. Hamila, "Literature review of advancements in adaptive ramp metering," in *Proceedings of the 7th International Conference on Ambient Systems, Networks and Technologies, ANT 2016 and the 6th International Conference on Sustainable Energy Information Technology*, pp. 203–211, SEIT, 2016. Spain, May 2016.

[4] W. Xin, P. Michalopoulos, J. Hourdakis, and D. Lau, "Minnesota's new ramp control strategy design overview and preliminary assessment," *Transportation Research Record*, vol. 1867, pp. 69–79, 2004.

[5] I. Papamichail and M. Papageorgiou, "Traffic-responsive linked ramp-metering control," *IEEE Transactions on Intelligent Transportation Systems*, vol. 9, no. 1, pp. 111–121, 2008.

[6] K. H. S. Mohammad and A. Kondyli, "Evaluation of ramp metering impacts on travel time reliability and traffic operations through simulation," *Journal of Advanced Transportation,*, vol. 2019, pp. 1–12, 2019.

[7] S. Ahn, R. Bertini, B. Aufray, J. Ross, and O. Eshel, "Evaluating benefits of systemwide adaptive ramp-metering strategy in portland, oregon," *Transportation Research Record*, no. 2012, pp. 47–56, 2007.

[8] M. Abdel-Aty, A. Pande, C. Lee, V. Gayah, and C. Santos, "Crash risk assessment using intelligent transportation systems data and real-time intervention strategies to improve safety on freeways," *Journal of intelligent transportation systems*, vol. 11, no. 3, pp. 107–120, 2007.

[9] D. Gettman, *A multi-objective integrated large-scale optimized ramp metering control system for freeway/surface-street traffic management*. ISBN: 0599104007; ISBN: 9780599104006: ProQuest Dissertations Publishing, 1998.

[10] Y. Han, M. Ramezani, A. Hegyi, Y. Yuan, and S. Hoogendoorn, "Hierarchical ramp metering in freeways: An aggregated modeling and control approach," *Transportation Research Part C: Emerging Technologies*, vol. 110, pp. 1–19, 2019.

[11] R. Jiang, J. Lee, and E. Chung, "A multi-hierarchical strategy for on-ramp coordination," *International Journal of ITS research*, vol. 15, no. 1, pp. 50–62, 2017.

[12] A. Kotsialos and M. Papageorgiou, "The importance of traffic flow modeling for motorway traffic control," *Networks and spatial economics,*, vol. 1, no. 1, pp. 179–203, 2001.

[13] F. Marczak, L. Leclercq, and C. Buisson, "A macroscopic model for freeway weaving sections," *Computer-aided civil and infrastructure engineering*, vol. 30, no. 6, pp. 467–477, 2015.

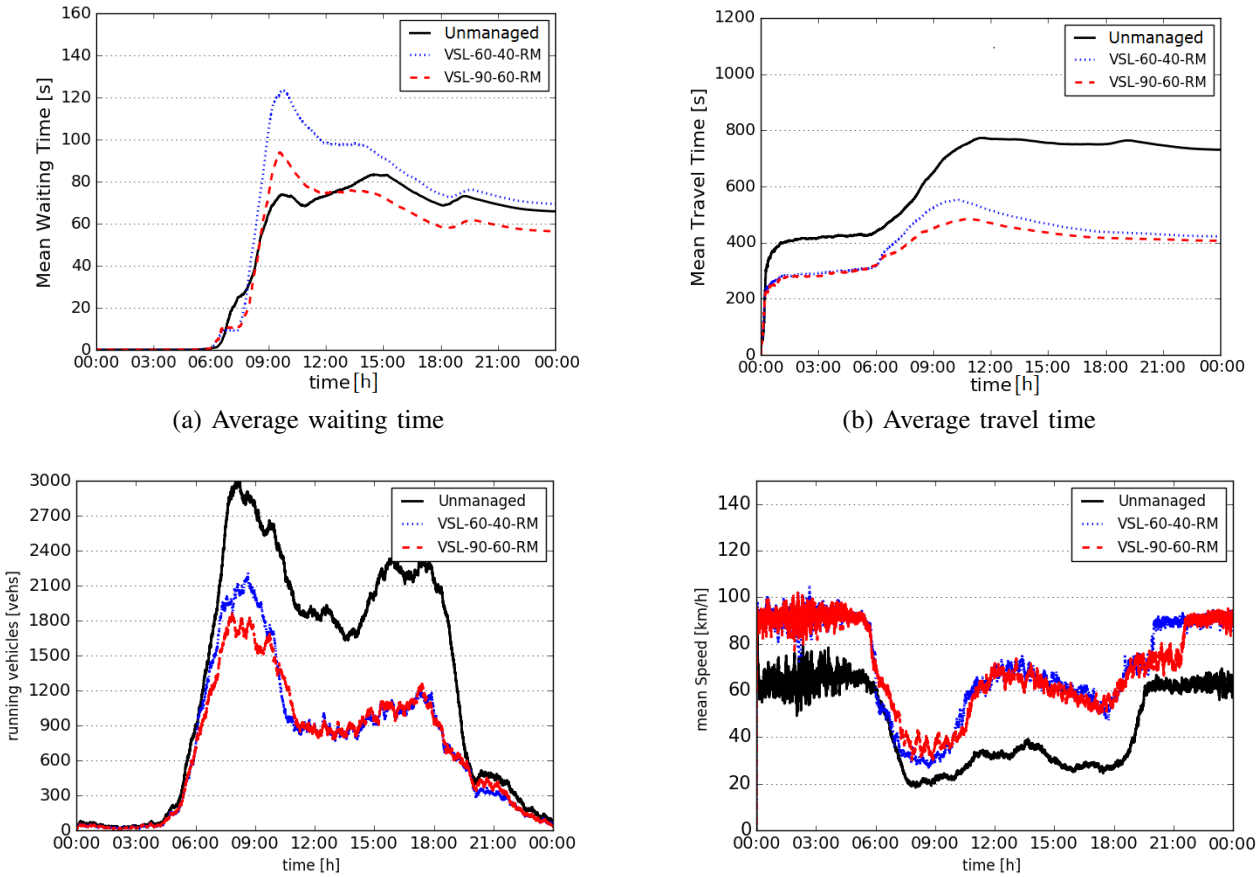

(a) Average waiting time

(b) Average travel time

(c) Average running vehicles

(d) Average speed

Fig. 4. Effect of three control strategies on road capacity: (a) average waiting time; (b) average travel time; (c) average running vehicles; (d) average speed.

[14] M. Papageorgiou, J.-M. Blosseville, and H. Haj-Salem, "Modelling and real-time control of traffic flow on the southern part of boulevard peripherique in paris: part ii: coordinated onramp metering," *Transportation Research Part A: General*, vol. 24, no. 5, pp. 361–370, 1990.

[15] J. Xu, X. Zhao, and D. Srinivasan, "On optimal freeway local ramp metering using fuzzy logic control with particle swarm optimisation," *IET intelligent transport systems*, vol. 7, no. 1, pp. 95–104, 2013.

[16] G. Zhang and Y. Wang, "Optimizing coordinated ramp metering: A preemptive hieracrhical control approach," *Computer-aided civil and infrastructure engineering*, vol. 28, no. 1, pp. 22–37, 2013.

[17] I. Abuamer, M. Silgu, and H. Celikoglu, "Micro-simulation based ramp metering on istanbul freeways : An evaluation adopting alinea," in *2016 IEEE 19th International Conference on Intelligent Transportation Systems (ITSC)*, pp. 695–700, 2016. https://doi.org/10.1109/ITSC.2016.7795629.

[18] N. Amini, H. Grzybowska, K. Wijayaratna, and S. Waller, "Systemic evaluation of the hero-based ramp metering algorithm using microsimulation," in *2015 IEEE 18th International Conference on Intelligent Transportation Systems*, pp. 2287–2292, IEEE Xplore, 2015. doi: 10.1109/ITSC.2015.369.

[19] R. Carlson, I. Papamichail, M. Papageorgiou, and A. Messmer, "Optimal motorway traffic control involving variable speed limits and ramp metering," *Transportation science*, vol. 44, no. 2, pp. 238–253, 2015.

[20] L. Chu, H. Liu, W. Recker, and H. Zhang, "Performance evaluation of adaptive ramp-metering algorithms using microscopic traffic simulation mode," *Journal of Transportation Engineering*, vol. 130, pp. 330–338, 2004.

[21] O. Minoarivelo, *Application of Markov Decision Processes to the Control of a Traffic Intersection*. Postgraduate diploma, University of Barcelona, 2009.

[22] S. Krauβ, *Microscopic Modelling of Traffic Flow: Investigation of Collision Free Vehicle Dynamics*. ISBN: 1434-845: Hauptabteilung Mobilität und Systemtechnik des DLR Köln, 1998.

[23] V. Jordanoska, I. Gjurkov, and D. Danev, "Comparative analysis of car following models based on driving strategies using simulation approach," *Mobility and Vehicle Mechanics,*, vol. 44(3), pp. 1–11, 2018.

[24] C.-J. Jin, R. Jiang, H.-F. Liang, D. Li, and H. Wang, "The similarities and differences between the empirical and experimental data: investigation on the single-lane traffic," *Transportmetrica B: Transport Dynamics*, vol. 7, no. 1, pp. 1323–1337, 2019.

[25] S. Haddouch, H. Hachimi, and N. Hmina

[26] D. Krajzewicz, J. Erdmann, M. Behrisch, and L. Bieker-Walz, "Recent development and applications of sumo - simulation of urban mobility," *International Journal On Advances in Systems and Measurements*, vol. 3&4, 12 2012.

[27] L. Bieker-Walz, D. Krajzewicz, A. Morra, C. Michelacci, and F. Cartolano, "Traffic simulation for all: A real world traffic scenario from the city of bologna," *Lecture Notes in Control and Information Sciences*, vol. 13, pp. 47–60, 01 2015.

[28] Z. Liu, Y. Wu, S. Cao, L. Zhu, and G. Shen, "A ramp metering method based on congestion status in the urban freeway," *IEEE Access*, vol. 8, pp. 76823–76831, 2020.

[29] L. Urquiza-Aguiar, W. Coloma-Gómez, P. Bautista, and X. Calderón-Hinojosa, "Comparison of sumo's vehicular demand generators in vehicular communications via graph-theory metrics," *Ad Hoc Networks*, vol. 106, p. 102217, 2020.

[30] J. Zambrano-Martinez, C. Calafate, D. Soler, and J.-C. Cano, "Towards realistic urban traffic experiments using dfrouter: Heuristic, validation and extensions," *Sensors*, vol. 17, no. 12, 2017.